University of Groningen

Fast-moving dislocations in high strain rate deformation

Roos, Arjen

IMPORTANT NOTE: You are advised to consult the publisher's version (publisher's PDF) if you wish to cite from it. Please check the document version below.

Document Version
Publisher's PDF, also known as Version of record

Publication date:
1999

Link to publication in University of Groningen/UMCG research database

Citation for published version (APA):
Roos, A. (1999). *Fast-moving dislocations in high strain rate deformation*. s.n.

CHAPTER 3

DISLOCATION DRAG MECHANISMS

§3.1 INTRODUCTION

HIGH STRAIN RATE deformation of materials is commonly described by so-called constitutive equations which link *macroscopic* strain (γ), strain rate ($\dot{\gamma}$) and temperature (T) with *macroscopic* stress (τ). Because plastic deformation is in essence an irreversible and consequently a path-dependent process, the mechanical response of a material also depends on the deformation substructures created *during the process*. Depending on $\dot{\gamma}$, T and the stress state, however, a variety of substructures exists and therefore one has to add the deformation history to the constitutive equations. The latter is usually neglected, but not in our case:

$$\tau = f\left(\gamma, \dot{\gamma}, T, \text{deformation history}\right) \qquad (3.1–1)$$

In the following sections we will discuss plasticity and the accompanying drag mechanisms on the dislocation level. To make a connection with the constitutive equation it is appropriate to summarise some of its essentials.

There are quite a number of constitutive equations proposed, and indeed successfully applied, to describe plastic deformation. The basic idea is to collapse all the mechanical data into one single equation. The main ingredients are based on the well-known power law

$$\tau = \tau_0 + k\gamma^n, \qquad (3.1–2)$$

(with n the work-hardening coefficient and k and τ_0 constants), and a description of the effect of temperature on the flow stress:

$$\tau = \tau_R \left[1 - \left(\frac{T - T_R}{T_M - T_R} \right)^m \right],$$
(3.1–3)

with T_M the melting temperature and T_R a reference temperature at which the reference stress τ_R is measured. The effect of strain rate can often simply be approximated by

$$\tau \sim \ln\left(\dot{\gamma}/\dot{\gamma}_0\right),$$
(3.1–4)

although this description breaks down at strain rates above $10^2\ \mathrm{s}^{-1}$.

These basic ingredients were combined by Johnson et al.[1] leading to

$$\tau = \left(\tau_0 + B\gamma^n\right)\left(1 + C\ln\left[\frac{\dot{\gamma}}{\dot{\gamma}_0}\right]\right)\left(1 - \left[\frac{T - T_R}{T_M - T_R}\right]^m\right).$$
(3.1–5)

Equation (3.1–5) turns out to be very successful and the parameters τ_0, B, C, n and m are determined for a number of materials and even, in a modified form, for ceramics[2]. In addition, the Johnson equation is stretched so as to incorporate dynamic recrystallisation at higher temperatures[3]. It is important to realise that the constitutive equations are basically "curve-fitting" procedures and that several research groups have developed their own functional form. For example, the following functional dependence was successfully applied to Cu[4]:

$$\tau = A\gamma^n\left(1 + m\ln\left[1 + \frac{\dot{\gamma}}{B}\right]\right),$$
(3.1–6)

with A, B, n and m constants. Nevertheless, to make reasonable estimates of certain specific material behaviour, these rather empirical constitutive equations are still useful (for example to estimate the temperature rise during high strain rate deformation, see Chapter 5 and Chapter 6).

Another important aspect in our work on discrete dislocation plasticity is the relation between resolved shear stress σ experienced by the dislocation, and dislocation velocity v_{DIS}. For this we have to start with Newton's second law of motion and define the force exerted on a dislocation. A general expression for this force can be found readily: if a dislocation segment $\mathrm{d}\vec{\xi}$ moves a distance $\mathrm{d}\vec{s}$ under the applied stress tensor $\vec{\vec{\Sigma}}$, the amount of work done is

$$dW = \left(d\vec{\xi} \times d\vec{s}\right)\vec{\vec{\Sigma}} \cdot \vec{b} , \qquad (3.1-7)$$

where $\vec{b}$ denotes the Burgers vector. With a *symmetric* stress tensor $\vec{\vec{\Sigma}}$, the work done can be written as

$$dW = \vec{b}\vec{\vec{\Sigma}} \cdot \left(d\vec{\xi} \times d\vec{s}\right) = \left(\vec{b}\vec{\vec{\Sigma}} \times d\vec{\xi}\right) \cdot d\vec{s} , \qquad (3.1-8)$$

or, using $dW = d\vec{F} \cdot d\vec{s}$,

$$d\vec{F} = \left(b\vec{\vec{\Sigma}}\right) \times d\vec{\xi} . \qquad (3.1-9)$$

The stress tensor $\vec{\vec{\Sigma}}$ represents the sum of all the fields of the strings of dislocations (~) and the correction fields (^) (see section 2.3). This equation is called the *Peach-Köhler equation* From now on, we will denote the *local* resolved shear stress on the dislocation by σ_{PK}. In all cases referring to a *local* quantity (for instance, the strain component ε_{12} of an edge dislocation), the coordinate system is oriented with respect to the dislocation as in figure 2.2−1. The contributions to σ_{PK} may be the stress fields of other dislocations and obstacles, and the *local* component of the *macroscopic* applied stress τ. For an edge dislocation, the Peach-Köhler force $F_{\text{Peach-Köhler}}$ then reduces to $\sigma_{PK}b$.

Also in this case, various semi-empirical approaches do exist in literature. Based on "curve-fitting" procedures the dislocation velocity-stress dependence is commonly described by[5,6]

$$v_{\text{DIS}} = A\left(\sigma_{PK}\right)^{m} e^{-E/k_{B}T} , \qquad (3.1-10)$$

or in simple form[7]:

$$v_{\text{DIS}} = v_{0}\left(\frac{\sigma_{PK}}{\sigma_{PK}^{0}}\right)^{m} . \qquad (3.1-11)$$

The difficulty with these expressions is that there is no upper limit for v_{DIS} as a function of σ_{PK}. Gilman[8] repairs this by writing

$$v_{\text{DIS}} = v_{A}e^{-\frac{A}{\sigma_{PK}}} + v_{B}\left(1 - e^{-\frac{\sigma_{PK}}{B}}\right), \qquad (3.1-12)$$

with A and B constants, and v_A and v_B limiting velocities for $\sigma_{PK} \to 0$ and $\sigma_{PK} \to \infty$, respectively. At moderate stresses the dislocation velocity is proportional to the applied stress. This can be used in the determination of the dislocation damping coefficient B.

Returning to Newton's second law and assuming a linear proportionality between the stress and the dislocation velocity, it would mean

$$\sigma_{PK} \propto a \quad \text{and} \quad v_{DIS} \propto a, \tag{3.1–13}$$

with a the acceleration. The two expressions (3.1–13) combined would imply that the dislocation undergoes an *acceleration* under a *constant velocity* at a certain stress. This is clearly a contradiction. To "hold back" the dislocation, there are two possibilities:
(a) there is a drag damping the motion of the dislocation. This drag is considered viscous, in analogy with the movement of a body through a fluid)
(b) the mass increases with velocity causing the acceleration to decrease upon increasing velocity.

Furthermore, there exist various kinds of obstacles to the motion of dislocations. In fact, these obstacles control the flow stress to a great extent at relatively low strain rate deformations. There are even so-called thermal obstacles that can be released under the influence of a stress that is smaller than the glide resistance of the obstacles. This is expressed by an Arrhenius equation

$$v_{DIS} = v_0 \, e^{-\frac{\Delta G}{kT}}, \tag{3.1–14}$$

and leads to a third regime
(c) dislocation dynamics described by thermally activated dislocation motion.

In the following sections, the three governing mechanisms of thermally activated dislocation motion, dislocation drag and relativistic effects will be scrutinised as a function of the dislocation velocity and strain rate. This will be delineated with increasing deformation rate in the sequence: thermally activated dislocation motion, dislocation drag, relativistic regime.

§3.2 THERMALLY ACTIVATED MOTION

Apart from the Peierls-Nabarro stress resisting the initiation of dislocation motion, other obstacles may be dispersed in the lattice, for instance solute atoms, precipitates, other dislocations etc. The impediment of the motion may also have its origin in the moving dislocation itself (by cross slip, or jog formation). Which of

these obstacles are predominant depends on their strength, the temperature, the external stress, etc.

In overcoming an obstacle, free energy may be stored *temporarily* (e.g. by increased dislocation length) or *permanently* (e.g. by the creation of jogs after intersection). Processes of the former kind can be thermally activated, while the latter processes cannot. Consequently, the macroscopic shear stress may be divided in an *a-thermal* part connected to structure, and a *thermal* part. In the literature it is sometimes called the *internal stress*, because it arises from the "internal" stress due to other dislocations. However, we do not support this idea because the resistance of bowing out a dislocation loop is due to its own *line tension* and *not* to the *internal stress*. Decisive for the a-thermal stress is whether it is of long-range nature, in which case it cannot be overcome by thermal activation. Consequently, under the influence of an external applied stress an *effective* stress (i.e. the applied stress corrected for the structural part) is available to move a dislocation across a barrier.

The principal short-range barrier, i.e. the Peierls-Nabarro stress, is important for bcc metals but not for our case, fcc and hcp materials. For fcc and hcp metals, dislocation forest dislocations are the primary short-range barriers at lower temperatures.

The rather empirical equation (3.1−14) is only useful if the rate determining processes are of "atomic dimension" (i.e. of short-range nature), for example in the diffusion process which is determined by the jumping atoms. Furthermore, the activation event in deforming crystals, proceeding under the influence of (external) stresses should be independent of temperature if the stresses are equal or larger than a maximum opposing stress. Therefore ΔG is stress-dependent.

Kocks et al.[9] discuss the vibrational frequency of dislocations and conclude $\nu_0 = 10^{11}$ s^{-1}, about two orders of magnitude smaller than the vibrational frequency of atoms $\nu_D = 10^{13}$ s^{-1}. The lower bound of ν_0 is related to the spacing l between the obstacles:

$$\nu_0 = \nu_D \frac{b}{4l}. \qquad\qquad (3.2-1)$$

For an annealed metal with dislocation density of 10^{11}–10^{12} m^{-2}, equation 3.2−1 yields $\nu_0 \cong 10^9$ s^{-1}.

Equations (3.1−14) and (3.2−1) still cannot explain for the fact that macroscopic deformation of a crystal starts at a certain critical flow stress. In the description of thermally activated motion at stresses below a certain mechanical threshold, the progress of a dislocation through the crystal over its glide plane is jerky[10]. Dislo-

cations are assumed to move between obstacles during a relatively short time interval τ_{RUN}. During the waiting time τ_{WAIT} at obstacles they may be released either by thermal fluctuations, by a change in the applied stress, or by a change in the obstacle structure. If it is assumed that no obstacles are present, that all dislocations move on one singular slip plane and remain straight, and that their velocity v_{DIS} is determined by an effective applied stress, and that this is the same for every moving dislocation, then the transport equation of the shear strain rate

$$\dot{\gamma} = b\rho_{\mathrm{M}}\bar{v}_{\mathrm{DIS}} \qquad (3.2\text{--}2)$$

(the so-called *Orowan equation*, which connects the *macroscopic* strain rate to *microscopic* quantities) describes the process of continuous glide, in which at any instant *all* dislocations are mobile ($\rho_{\mathrm{M}} = \rho_{\mathrm{TOT}}$ denotes the density of *mobile* dislocations). In the case of jerky glide, the macroscopic strain rate is provided *only* by those dislocations which are running, and

$$\dot{\gamma} = b\rho_{\mathrm{RUN}}\bar{v}_{\mathrm{RUN}} , \qquad (3.2\text{--}3)$$

where ρ_{RUN} is the density of the running dislocations. The running dislocations are transferred from the waiting state to the running state by release at the obstacle at a rate $\rho_{\mathrm{WAIT}}\dot{P}$. Here $\dot{P}$ denotes the fraction released per unit time under a thermal fluctuation (or a fluctuation in external or internal stress), and ρ_{WAIT} the density of dislocations trapped in front of an obstacle.

After travelling a distance L, the mean free path, the dislocations are transferred back to the waiting state and the kinetic balance reads

$$\dot{\rho}_{\mathrm{RUN}} = \rho_{\mathrm{WAIT}}\dot{P} - \frac{\rho_{\mathrm{RUN}}\bar{v}_{\mathrm{RUN}}}{L} = \rho_{\mathrm{WAIT}}\dot{P} - \frac{\rho_{\mathrm{RUN}}}{\tau_{\mathrm{RUN}}} , \qquad (3.2\text{--}4)$$

with solution

$$\rho_{\mathrm{RUN}} = \rho_{\mathrm{WAIT}}\dot{P}\tau_{\mathrm{RUN}}\left(1 - e^{-\frac{t}{\tau_{\mathrm{RUN}}}}\right). \qquad (3.2\text{--}5)$$

After $t \gg \tau_{\mathrm{RUN}}$, when steady state between waiting and running densities has been reached, $\dot{\rho}_{\mathrm{RUN}} = 0$ and equation (3.2–3) becomes

$$\dot{\gamma} = bL\rho_{\mathrm{WAIT}}\dot{P} . \qquad (3.2\text{--}6)$$

If $\rho_{\mathrm{TOT}} = \rho_{\mathrm{WAIT}} + \rho_{\mathrm{RUN}}$ is constant, then

$$\dot{\gamma} = b\rho_{\mathrm{M}} \frac{L}{\tau_{\mathrm{WAIT}} + \tau_{\mathrm{RUN}}} . \qquad (3.2–7)$$

Usually, $\tau_{\mathrm{WAIT}} \gg \tau_{\mathrm{RUN}}$ and

$$\dot{\gamma} = b\rho_{\mathrm{M}} \frac{L}{\tau_{\mathrm{WAIT}}} . \qquad (3.2–8)$$

The mobile dislocation density ρ_{M} can be estimated from the experimentally known fraction of the total ρ_{TOT}, which is about[10] 0.25. With strain rates up to $1\ \mathrm{s}^{-1}$, and $\rho_{\mathrm{TOT}} \sim 10^{12}\ \mathrm{m}^{-2}$ and obstacles spaced about 1 μm apart, the mean waiting time τ_{WAIT} becomes $2.5 \cdot 10^{-4}$ s. This average waiting time is governed by the probability that an obstacle will be overcome by thermal fluctuations, see equation (3.1–14), according to

$$\frac{1}{\tau_{\mathrm{WAIT}}} = \nu = \nu_0 e^{-\frac{\Delta G}{k_{\mathrm{B}} T}} , \qquad (3.2–9)$$

or by equation 3.2–1:

$$\frac{1}{\tau_{\mathrm{WAIT}}} = \nu_{\mathrm{D}} \frac{b}{4l} e^{-\frac{\Delta G}{k_{\mathrm{B}} T}} . \qquad (3.2–10)$$

Using $\tau_{\mathrm{WAIT}} = 2.5 \cdot 10^{-4}$ s in equation (3.2–10) and $\nu_{\mathrm{D}} = 10^{10}\ \mathrm{s}^{-1}$, an activation energy of about 0.3 eV is found, which is a reasonable value in an atomistic picture. In the regime where $\tau_{\mathrm{RUN}} > \tau_{\mathrm{WAIT}}$ we have to turn to another relationship between dislocation velocity and applied stress as will be explained in the next section.

§3.3 DISLOCATION DRAG MECHANISMS

In this second regime the velocity of the dislocations is proportional to the applied stress, that is to say the exponent in equation (3.1–11) is equal to one[9]. This means that the solid acts as a Newtonian viscous material:

$$\vec{F}_{\mathrm{drag}} = -B\vec{v}_{\mathrm{DIS}} , \qquad (3.3–1)$$

where B represents the damping coefficient and the minus sign signifies that the drag force works in the direction opposite to the motion. In a Newtonian viscous material, the damping coefficient does *not* depend on the velocity v_{DIS}. Writing the

force balance of the straight dislocation line (neglecting inertial effects for now) and substituting the Peach-Köhler force from equation 3.1−9 yields

$$F_{\text{Peach−Köhler}} + F_{\text{drag}} = 0 \quad \Leftrightarrow \quad \sigma_{\text{PK}}\, b = B\, v_{\text{DIS}}, \tag{3.3−2}$$

It is easy to see that under steady-state conditions (see equation (3.2−2)), the flow stress should be proportional with the *macroscopic* strain rate $\dot{\gamma}$ if dislocation drag mechanisms are operative. Indeed, most of the mechanical energy applied to the material is dissipated by forces opposing the applied stress. In fact, macroscopically only about 10% is residually stored as defects in the substructures. At a *local* scale of a moving dislocation this is not relevant and one may argue that *all* the mechanical energy is dissipated in the form of heat (see Chapter 5).

To a first approximation the drag coefficient $B = B_{\text{TOT}}$ consists of three basic contributions

$$B_{\text{TOT}} = B_{\text{PH}} + B_{\text{E}} + B_{\text{IMP}}, \tag{3.3−3}$$

where the subscripts PH, E and IMP refer to phonon viscosity, electron viscosity and impurity effects, respectively. In addition, one may think of other contributions[11], such as magnon drag in magnetic crystals, but we will not treat these here. In the following sections, we will consider each contribution to equation (3.3−3) separately.

3.3.1 PHONON VISCOSITY

Dislocations moving in the flux of phonons experience frictional forces. In the late sixties and early seventies, many a paper (for instance in refs. 11−16) was devoted to identify the separate processes contributing to the total force. The picture that eventually emerged is briefly summarised below.

The terms contributing to phonon damping may be grouped according to whether the dislocation line is considered *flexible* or *rigid*. In the first case, the thermal phonons excite vibrations in the dislocation line, which are then re-radiated in a cylindrical wave around the dislocation line. When the dislocation is moving, this gives rise to a net force opposing the motion. This is called the *flutter mechanism* and it is described in terms of linear elasticity[17]. The resulting drag coefficient is denoted by B_{flut}. At low temperatures ($T \ll \theta_{\text{D}}$, with θ_{D} the Debye temperature), its temperature dependence follows T^3, while at higher temperatures the dependence is linear. We will come back to this contribution later in this section.

Further, if accelerations and decelerations are involved, dislocations emit elastic waves corresponding to the outflow of energy. The amount of radiated energy is

proportional the rate of change of the resolved shear stress on the dislocation. One cause is the periodic change in velocity due to the interaction with the Peierls hills (in particular for motion in bcc lattices), but at high velocities this contribution becomes negligibly small, and we will neglect it. However, it is not clear *a priori* whether we may neglect the accelerations due to a change in applied stress, and we will turn our attention to this question in sections 3.4, 4.3 and 6.2.1. In the discussion of the next two sections, we will confine ourselves therefore to dislocation motion at *constant velocity*.

In the second group, where the dislocation is considered rigid, it cannot scatter phonons by fluttering. However, close to the dislocation core, linear elasticity ceases to be valid, and the phonons are scattered by *anharmonicities* in the strain field[12–15]. Once more, a moving dislocation encounters more phonons in the direction of motion than in other directions (giving rise to the so-called *phonon wind*), and the resulting drag coefficient is called B_{wind}. At low temperatures, it is proportional to T^5, while at high temperatures, $B_{wind} \propto T$ (as in the case of the flutter mechanism). The following expressions were derived by Brailsford[13]:

$$B_{wind}^0 = \frac{384\alpha_G^2\hbar}{b^3}\left(\frac{a_2}{a_1}\right)^4\left(\frac{q_D b}{2\pi}\right)^5\left(\frac{T}{\theta_D}\right)^5 \quad \text{for } T \ll \theta_D \qquad (3.3\text{–}4)$$

and

$$B_{wind}^0 = \frac{96\alpha_G^2\hbar}{b^3}\left(\frac{a_2}{a_1}\right)^4\left(\frac{q_D b}{2\pi}\right)^5\frac{T}{\theta_D} \quad \text{for } T \geq \theta_D \qquad (3.3\text{–}5)$$

with α_G the Grüneisen parameter (which also depends on temperature). The superscript 0 stresses the fact that this coefficient does *not* depend on the dislocation velocity v_{DIS}.

The *thermo-elastic* effect is related to the concept that a moving dislocation strains adjacent regions in tension and compression. It can be seen that the accompanying temperature change falls and rises (respectively) inversely proportional with the distance to the dislocation (Chapter 6). This in turn leads to a change in entropy. Consequently, energy is depleted from the dislocation, leading to a contribution B_{TE}^0 proportional to $c_V(T)T \ln(a_2/v_{DIS})$, with c_V the specific heat at constant volume. Because of this effect, the area in front of a moving dislocation is not only heated but at some larger distances also cooled. This term may gain relative importance at high temperatures ($T \gg \theta_D$), because then $B_{TE} \propto T^2$. In metals, however, it is usually neglected[13,14].

The last, but important, contribution is that due to so-called slow phonons, where the term slow refers to the group velocity. This interaction arises due to the devia-

tion from linearity of the dispersion in a real crystal and was first suggested by Al'shitz and Indenbom[12]. The point is that the phonon viscosity is related to the density of phonon modes per unit frequency range, $D(\omega)$. The latter is inversely proportional to the group velocity $d\omega/dk$. It is clear that there will be a singularity in $D(\omega)$ whenever the dispersion relation $\omega(k)$ becomes horizontal; that is to say, whenever the group velocity become zero. In a part of the k-space, e.g. in the vicinity of the Brillouin zone boundary, the group velocity may be reduced and the phonons are literally slow.

At the Debye temperature and higher, the magnitude of this contribution to phonon viscosity becomes constant and is comparable to B_{flut}. It is given by

$$B_{\text{slow}}^0 = \frac{\alpha^2 \hbar b^2 q_{\text{D}}^4}{8\pi^5 r_0},$$

(3.3–6)

where r_0 is of the size of the dislocation core radius, and α is a numerical factor[11], depending on the particular anharmonic model in use. For the Gruneisen model, it equals the Grüneisen parameter α_{G}, but in the literature, some other models are also employed[12]. The superscript 0 again stresses the fact that this coefficient does not depend on the dislocation velocity v_{DIS}. However, the actual contribution of B_{slow}^0 to the phonon viscosity depends critically on the details of the phonon spectrum of the specific material investigated. For fcc materials the inter-atomic interactions can be thought to be effectively projected onto the first nearest neighbour. Actually, the first nearest neighbour interactions seem to dominate at least up to sixth neighbours. In the limit of first nearest neighbour (harmonic) interactions, ω depends sinusoidally on k. Consequently, near the boundary of the first Brillouin zone there are no flat regions by which the group velocity is reduced, and effectively the Brillouin zone is replaced by a sphere. In the case of fcc materials only small flat areas in side the Brillouin zone can be found, in sharp contrast to bcc materials. Therefore we anticipate that B_{slow}^0 yields a substantial contribution to the total phonon viscosity for bcc and less for fcc materials. Nevertheless, if the flat region occupies already a relative volume of $r_o/l(\theta_{\text{D}})$ in the first Brillouin zone (where $l(\theta_{\text{D}})$ is the phonon mean free path at θ_{D}) the slow phonon relaxation contributes a substantial amount[12], in Cu a relative volume of already 1%.

In summary, the phonon drag term is

$$B_{\text{PH}} = B_{\text{wind}}^0 + B_{\text{flut}} \quad \text{at } T \ll \theta_{\text{D}}$$

(3.3–7)

and

$$B_{\text{PH}} = B_{\text{wind}}^0 + B_{\text{flut}} + B_{\text{slow}}^0 \quad \text{at } T \geq \theta_{\text{D}}.$$

(3.3–8)

In all interactions with the phonons of the strain field of the moving dislocation, the field of the static approximation ($v_{DIS} \to 0$) of equations (2.2–12) and (2.2–13) has been used, even for dislocation velocities approaching the lowest velocity of sound. In the following, we will investigate whether the high-velocity fields lead to a relativistic contribution to the damping terms. Note that this leads to a velocity-*dependent* (i.e. non-Newtonian) drag coefficient. Since our description is linear elastic, we will consider the fluttering mechanism. In this mechanism, a dislocation in translational motion interacts with phonons via elastic scattering accompanying momentum transfer. The latter gives rise to the inertia of dislocation motion, that is to say a retarding force. The starting point in our description is therefore the total momentum of the phonon gas

$$\vec{p} = \sum \hbar \vec{k} N(\vec{k}),$$
(3.3–9)

where $N(\vec{k})$ is the number of phonons in a vibrational mode $\{\vec{k}\}$. Because of the interaction between moving dislocations and elastic waves, phonons are interchanged between the various modes which leads to a variation of the occupation number $N(\vec{k})$. The average retarding force is then

$$\vec{f} = -\sum \hbar \vec{k} \; \dot{\overline{N}}(\vec{k}).$$
(3.3–10)

The rate of change of the average numbers of phonons $\overline{N}(\vec{k})$ in mode $\{\vec{k}\}$ can be expressed in a general form[18]

$$\dot{\overline{N}}(\vec{k}) = \sum W(\vec{k}, -\vec{k}')[\overline{N}(\vec{k}') - \overline{N}(\vec{k})] + \cdots \quad .$$
(3.3–11)

The sum in equation (3.3–11) represents the increase per unit of time of the average number of phonons in mode $\{\vec{k}\}$ and $W(\vec{k}, -\vec{k}')$ is the probability rate for the scattering of a phonon from mode $\{\vec{k}\}$ to $\{\vec{k}'\}$. Next, we assume that the energy of the phonon gas is also conserved in three-phonon collisions, and $W(\vec{k}, \vec{k}', -\vec{k}'')$ vanishes.

For *static* defects one finds, according to Fermi's Golden Rule,

$$W_{static}(\vec{k}, -\vec{k}') = w_{static}(\vec{k}, -\vec{k}') \delta(\omega(\vec{k}) - \omega(\vec{k}'))$$
(3.3–12)

with

$$w_{static}(\vec{k}, -\vec{k}') = 2\pi \left[\frac{(2\pi)^3}{\Omega_0 \rho_0} \right]^2 \frac{|V_1(\vec{k}, -\vec{k}')|^2}{\omega(\vec{k})\omega(\vec{k}')} .$$
(3.3–13)

The delta function in (3.3–12) means that the energy of the phonons is conserved in collisions with *static* defects. W contains the basic physics of the description by V_1 which is the coupling between the vibrational modes, represented by $\{\vec{k}\}$, their polarisation vectors $\vec{e}(\vec{k})$ and the defects which are represented by the Fourier transforms $\Im(\varepsilon)$ of their strain fields ε. A typical element of V_1 has the form

$$V_1 = A_1\left(\vec{e}\cdot\vec{k}\right)\left(\vec{e}'\cdot\vec{k}'\right)\Im(\varepsilon)(\vec{q})+\cdots. \tag{3.3–14}$$

with $\vec{q}=(q_1,q_2,q_3)$. V_1 vanishes unless $\vec{k}+\vec{k}'+\vec{q}=0$, meaning that the momentum of the phonon is changed in collisions with the defects.

In our case of a *uniformly moving* dislocation, a standard time-dependent perturbation treatment yields the probability rate

$$W_{\text{moving}}\left(\vec{k},-\vec{k}'\right)= w_{\text{moving}}\left(\vec{k},-\vec{k}'\right)\delta\left(\omega(\vec{k})-\omega(\vec{k}')-(\vec{k}-\vec{k}')\cdot\vec{v}_{\text{DIS}}\right). \tag{3.3–15}$$

The latter reflects in the δ-function (compare equation 3.3–12), that after the interactions of the phonons with the defects not only the *momentum* changes but also the *energy*.

The static, i.e. dislocation velocity-*in*dependent, frictional coefficients due to the flutter effect are given in literature (where the superscript zero refers to the static limit) as[23]

$$B_{\text{flut}}^0 = \frac{k_\text{B}T\omega_\text{D}^2}{\pi^2 a_2^3}\quad\text{at high temperatures } T \geq \theta_\text{D} \tag{3.3–16}$$

and

$$B_{\text{flut}}^0 = \frac{14.4\,k_\text{B}T\omega_\text{D}^2}{\pi^2 a_2^3}\left(\frac{T}{\theta_\text{D}}\right)^2\quad\text{at low temperatures } T \ll \theta_\text{D}, \tag{3.3–17}$$

where ω_D is the Debye frequency corresponding to the Debye temperature $\theta_\text{D} = \hbar\,\omega_\text{D}/k_\text{B}$. At the low-temperature limit, the fluttering and non-linearity mechanism give drag coefficients of the same order of magnitude and at high temperatures their ratio becomes a constant with respect to temperature variations. However, we are interested here in the *velocity* dependence of the drag coefficients so as to use it over a large range of dislocation velocities.

We assume that the time the dislocation needs to travel a distance of the order of the phonon mean free path is *large* compared to the phonon relaxation time, i.e.

the phonon distribution is then, on average, equal tot the distribution in thermal equilibrium. The phonon relaxation time τ_{phonon} can be estimated from the thermal conductivity $K = c_V \rho v l / 3$, with c_V the specific heat and ρ the material density. With $v = a_2$, the phonon mean free path in Cu becomes $l_{\text{Cu}} \cong 40$ nm, yielding the relaxation time $\tau_{\text{phonon}} = l_{\text{Cu}}/a_2 \cong 10^{-11}$ s. If the dislocation velocity approaches the sound velocity the phonon distribution is *not* at an equilibrium

$$\overline{\overline{N}}_k^j = \left\{ \exp\left[\frac{\hbar \omega_k^j}{kT} \right] - 1 \right\}^{-1} , \tag{3.3−18}$$

and actually a heat current will arise from the deviations $\overline{N}\left(\vec{k}\right) - \overline{\overline{N}}\left(\vec{k}\right)$. This is basically also the difference between the thermal conductivity that can only exist provided $\overline{N}\left(\vec{k}\right) \neq \overline{\overline{N}}\left(\vec{k}\right)$ and the phonon drag which can exist even when $\overline{N}\left(\vec{k}\right) = \overline{\overline{N}}\left(\vec{k}\right)$.

It is rather difficult to work out analytical equations for the phonon-dislocation interactions in case the phonon distribution is not in thermal equilibrium. In general, to study the dissipative properties of a system it is convenient to apply the quantum-mechanical technique of non-equilibrium statistical mechanics. The dissipation of energy per unit time can be written as the product of the time derivative of the phonon Hamiltonian $H(t)$ and the deviation of the so-called density matrix, $\exp(-H(t)/T)/\text{Tr}\{\exp(-H(t)/T)\}$, from its equilibrium value. The latter can be expressed as a time dependent integral equation and accordingly the phonon-dislocation viscosity becomes time dependent. However, in the following we will assume only interactions of moving dislocations with a phonon gas in thermodynamic equilibrium, independent of t.

The velocity-dependent B_{flut} can now be found by taking the Fourier transform of the velocity-dependent strain fields and writing

$$B_{\text{flut}} = B_{\text{flut}}^0 f\left(v_{\text{DIS}} \right), \tag{3.3−19}$$

with $f(v_{\text{DIS}})$ the velocity-dependent part of the drag coefficient, and

$$B_{\text{flut}}^0 = \sum_{\vec{k}, \vec{k}'} \left| V_1\left(\vec{k}, \vec{k}', v_{\text{DIS}} \to 0 \right) \right|^2 \frac{\delta\left(\omega\left(\vec{k}\right) - \omega\left(\vec{k}'\right) \right)}{\omega\left(\vec{k}\right) \omega\left(\vec{k}'\right)}, \tag{3.3−20}$$

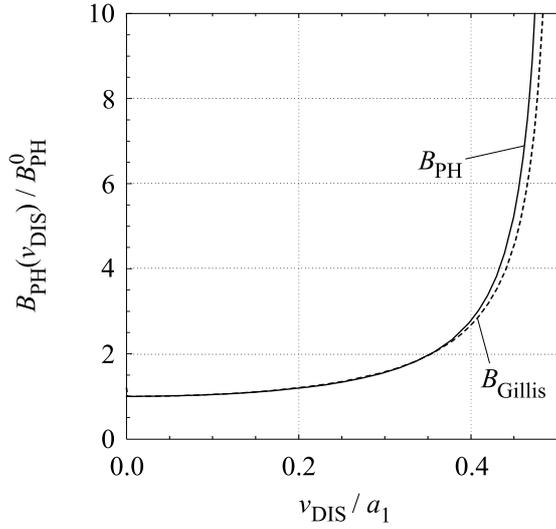which should agree with the static limits presented in equations (3.3−16) and (3.3−17).

FIGURE 3.3–1 Velocity-dependence $B_{PH}(v_{DIS})/B_{PH}^0$ of the phonon drag coefficient corresponding to the Fourier component due to ε_{12} (equation (3.3–22)) in a unit cell with cubic symmetry, and the Gillis-Gilman-Taylor drag coefficient (equation (3.3–23)) for $\nu = 1/3$ (or $a_1 = 2a_2$).

For glide in the positive or negative x_1-direction the relevant component of the (harmonic) strain field is the one due to ε_{12}. For an edge dislocation, it is given by

$$\varepsilon_{12} \equiv \frac{\partial u_1}{\partial x_2} + \frac{\partial u_2}{\partial x_1} = \frac{2b}{\pi} \frac{a_2^2}{v_{DIS}^2} \left\{ \frac{-\beta_1(x_1 - v_{DIS}t)}{(x_1 - v_{DIS}t)^2 + \beta_1^2 x_2^2} + \frac{\alpha^4}{\beta_2} \frac{(x_1 - v_{DIS}t)}{(x_1 - v_{DIS}t)^2 + \beta_2^2 x_2^2} \right\}$$

(equation (3.3–21)), where the displacement fields of equations (2.2–12) and (2.2–13) have been used. Its Fourier transform, which is taken in two dimensions (since all calculations take place in an essentially two-dimensional setting with straight dislocation lines), reads

$$\Im(\varepsilon_{12})(\vec{q}) = i\sqrt{\frac{2}{\pi}} \frac{\delta(q_3)e^{-iq_1 v_{DIS}t} b a_2^2}{v_{DIS}^2} \left\{ \frac{-\beta_1^2 q_2}{\beta_1^2 q_1^2 + q_2^2} + \frac{\alpha^4 q_2}{\beta_2^2 q_1^2 + q_2^2} \right\}, \qquad (3.3–22)$$

The velocity-dependence of the phonon drag coefficient due to ε_{12} is displayed in figure 3.3–1 for Cu. It is interesting to note that it agrees rather well with the empirical relation

$$B_{Gillis}(v_{DIS}) = \frac{B_{Gillis}^0}{1 - (v_{DIS}/a_2)^2} \qquad (3.3–23)$$

put forward by Gillis et al.[19], for which a detailed physical basis is provided here. Actually, the result of equations (3.3–22) and (3.3–23) can be obtained quite readily by realising that the drag coefficient is simply related to the ratio between

the momentum p_1 transferred per unit of area A (where the subscript 1 denotes the component of the momentum in the x_1-direction). According to special relativity theory, p_1 transforms to $p_1' = p_1/\beta_2$ and A transforms to $A' = \beta_2 A$ because of the Lorentz contraction. This leads immediately to equation (3.3–23) through

$$B = \frac{p_1'}{A'} = \frac{p_1}{\beta_2^2 A} = \frac{B_0}{1 - \left(v_{\text{DIS}}/a_2\right)^2} \qquad (3.3\text{–}24)$$

Because of its simplicity, we will take it as a basis for the further discussion of the dislocation velocity. It can be seen that viscous phonon drag increases as the dislocation velocity increases towards the shear wave velocity.

Collecting terms, the velocity dependence of the phonon drag coefficient finally becomes

$$B_{\text{PH}} = B_{\text{PH}}^{\text{static}} + B_{\text{PH}}(v_{\text{DIS}}) = \left(B_{\text{wind}}^0 + B_{\text{slow}}^0\right) + \frac{B_{\text{flut}}^0}{1 - \left(v_{\text{DIS}}/a_2\right)^2} \,, \qquad (3.3\text{–}25)$$

where the velocity-independent terms have been explicitly separated out from the velocity-dependent term. In principle, it should be possible to apply the procedure that was used to obtain the velocity-dependence of the flutter contribution, to the *an*harmonic contributions. When the higher order elastic constants are known, the anharmonic velocity-dependent displacements around the core can be derived in a similar manner as for the static case, based on the equations for the non-linear displacement fields[21]. These could then be used in the derivations of $B_{\text{wind}}(v_{\text{DIS}})$ and $B_{\text{slow}}(v_{\text{DIS}})$, as a function of the dislocation velocity. In this thesis, however, we will retain the static forms B_{wind}^0 and B_{slow}^0.

3.3.2 ELECTRON VISCOSITY

The interaction of moving dislocations with conduction electrons is attributed to the interaction of propagating elastic waves with the electrons. B_{E} can be derived from standard perturbation theory[21] or on the basis of the Boltzmann equation[22]. The latter development is briefly summarised here. The local lattice velocity $\dot{\vec{u}}(\vec{r},t)$, with $\vec{r} = (x_1, x_2, x_3)$ in the coordinate system as in figure 2.2–1, is described by

$$\dot{\vec{u}}(\vec{r},t) = \sum_q \vec{u}_q \, e^{i\vec{q}\cdot(\vec{r} - \vec{v}_{\text{DIS}}\,t)} \,, \qquad (3.3\text{–}26)$$

where

$$\vec{u}_q = \sum_\lambda -i\vec{q}\cdot\vec{v}_{DIS}\,\vec{e}_{q\lambda}\,\Im\vec{u}(\vec{r}-v_{DIS}t)_{q\lambda} \qquad (3.3\text{--}27)$$

with $q \equiv |\vec{q}|$ the wave number of the lattice wave and λ the normal mode with polarisation vector $\vec{e}_{q\lambda}$ (where $\lambda = 1$ denotes the longitudinal mode). Equation (3.3–27) contains the Fourier amplitude with lattice wave $\vec{q}$ of the displacement $\vec{u}(\vec{r})$. The latter is the displacement field of a *static* dislocation (i.e. the displacement fields of equations (2.2–12) and (2.2–13) in the limit $v_{DIS} \to 0$). The corresponding form for a *moving* dislocation with uniform velocity $\vec{v}_{DIS}$ is $\vec{u}(\vec{r}-\vec{v}_{DIS}t)$, provided $\vec{v}_{DIS}$ is small with respect to the sound velocity.

Taking the power dissipated by each component of equation (3.3–26) to be P_q,

$$P_q = A_\| \left|u_{q_\|}\right|^2 + A_\perp \left|u_{q_\perp}\right|^2 , \qquad (3.3\text{--}28)$$

where $\|$ and $\perp$ refer to the longitudinal ($\lambda = 1$) and transverse component, respectively, the effective drag force per unit length $B_E v_{DIS}$, leads to

$$B_E = \frac{1}{L v_{DIS}^2}\sum_q P_q , \qquad (3.3\text{--}29)$$

with L the length of the dislocation segment. Equation (3.3–29) should be evaluated in the limit $L \to \infty$. The theoretical problem thus reduces to the theoretical evaluation of $A_\|$ and $A_\perp$. Their electronic components have been calculated[23]:

$$A_\| \cong \frac{V n_0 m}{\tau}\frac{\pi q l_E}{6}\frac{1}{\left(1+(q/q_{TF})^2\right)^2} , \qquad (3.3\text{--}30)$$

with V the normalisation volume, n_0 the free electron density, m the electron mass, τ the relaxation time of the electrons, v_{FERMI} the velocity of electrons at the Fermi surface, $l_E = v_{FERMI}\tau$ the electron mean free path and q_{TF} the reciprocal Thomas-Fermi screening length ($q_{TF} = \sqrt{3}\,\omega_P/v_{FERMI}$ with $\omega_P^2 = n_0 e^2/\varepsilon_0 m$ the plasma frequency, e the electron charge and ε_0 the permittivity in vacuo). Substitution of equation (3.3–30) into (3.3–28) and (3.3–29) leads to

$$B_E^0 \cong \frac{\pi n_0 m v_{FERMI} V}{6 L v_{DIS}^2}\sum_q \frac{(\vec{q}\cdot\vec{v}_{DIS})^2\left|\Delta_q\right|^2}{q\left(1+(q/q_{TF})^2\right)^2} , \qquad (3.3\text{--}31)$$

where the superscript 0 denotes the fact that the *static* displacement fields have been used in the derivation of equation (3.3–31). Furthermore, $\Delta_q = i^3 q \Im(\vec{u})_{q1}$ is the Fourier component of the dilatation of an edge dislocation:

$$\Delta = \frac{\partial u_1}{\partial x_1} + \frac{\partial u_2}{\partial x_2} \,. \tag{3.3–32}$$

In equation (3.3–31) the transverse wave contribution is neglected because for $ql > 1$, $A_\perp \sim (ql)^{-1} A_\parallel$. For a screw dislocation in an isotropic linear elastic medium, $\Delta_q = 0$ and consequently $B_E^0 = 0$. In case of a straight edge dislocation lying along the x_3-direction with its Burgers vector pointing in the positive or negative x_1-direction Δ_q becomes

$$\Delta_q = \frac{2b}{V}\left(\frac{1-2\nu}{1-\nu}\right)\frac{\sin\left(\frac{1}{2}q_3 L\right)}{iq_3}\frac{q_2}{q_1^2 + q_2^2} \,. \tag{3.3–33}$$

Note that for this orientation of the straight edge dislocation, the direction of the glide velocity is in the $\pm x_1$-direction, so that in equation (3.3–31), $\vec{q} \cdot \vec{v}_{\mathrm{DIS}} = q_1 v_{\mathrm{DIS}}$. Finally, substitution of equation (3.3–33) into equation (3.3–31), replacing the summation by an integral and integrating over the Debye sphere of radius q_D yields

$$B_E^0 = \left(\frac{1-2\nu}{1-\nu}\right)^2 \frac{n_0 m v_{\mathrm{FERMI}} b^2 q_D}{96} \phi(q_D/q_{\mathrm{TF}}), \tag{3.3–34}$$

where $\phi(x) = \frac{1}{2}[(1+x^2)^{-1} + x^{-1}\arctan x]$. As an example, $B_E^0(\mathrm{Cu})$ is found to be 0.2 μPa s and $B_E^0(\mathrm{Al}) = 0.9$ μPa s.

It is important to note that this description of the electron viscosity leads to a temperature-*in*dependent contribution to the total drag. In addition, because the dilatation field was taken to be velocity-*in*dependent, equation (3.3–31) results in a velocity-*in*dependent contribution to the total drag coefficient. We will now investigate how this equation might be generalised to a *velocity-dependent* description, in an analogous fashion as for the flutter mechanism of the previous section. Note that this velocity-dependence is *not* based on the concept of electron viscosity, but rather on the velocity-dependent strain field.

In the derivation leading to equation (3.3–34) the following assumptions have been made:
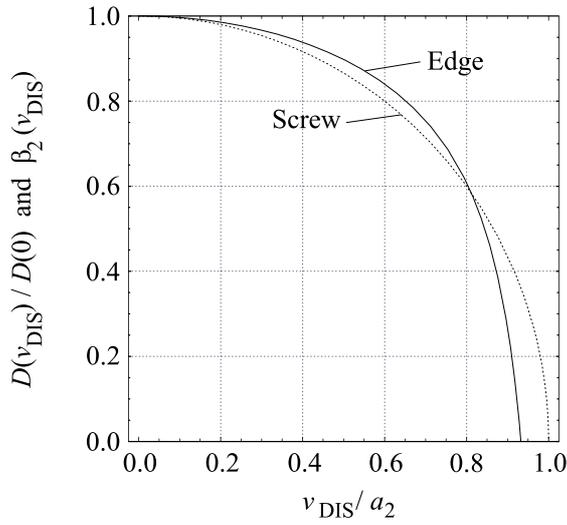
FIGURE 3.3–2 Velocity-dependent factor that modulates the width of the dislocation core in equation (3.3–38) (after Eshelby[25]).

$$ql \gg 1$$
$$\vec{v}_{\text{DIS}} \cdot \vec{q} \ll \sigma_0 \, , \tag{3.3--35}$$

where q denotes the magnitude of the 'typical' Fourier component of the strain field associated with the dislocation[13], and σ_0 the DC conductivity (in s^{-1}). The latter is of the order of 10^{16}–10^{17} s^{-1} for metals at room temperature[24]. The typical Fourier component may be related to the width of the dislocation, i.e. the extent of the core region that is not governed by linear elasticity. According to Eshelby[25], the width ζ of an edge dislocation is estimated to be

$$\zeta = \frac{a_{\text{L}}}{2(1-\nu)}, \tag{3.3--36}$$

where a_{L} is the lattice distance. The typical magnitude of q is then of the order

$$q = \frac{2\pi(1-\nu)}{a_{\text{L}}}. \tag{3.3--37}$$

In the velocity-dependent description, the width of the core varies as[25,26]

$$\zeta = \frac{a_{\text{L}}}{2(1-\nu)} \frac{D(v_{\text{DIS}})}{D(0)}, \tag{3.3--38}$$

with $D(v_{\text{DIS}}) = -2\mu(2a_2{}^2/v_{\text{DIS}}{}^2)(\beta_1 - \alpha^4/\beta_2)$. The width of the core of a screw dislocation varies with β_2. The velocity-dependent terms $D(v_{\text{DIS}})/D(0)$ and β_2 are dis-
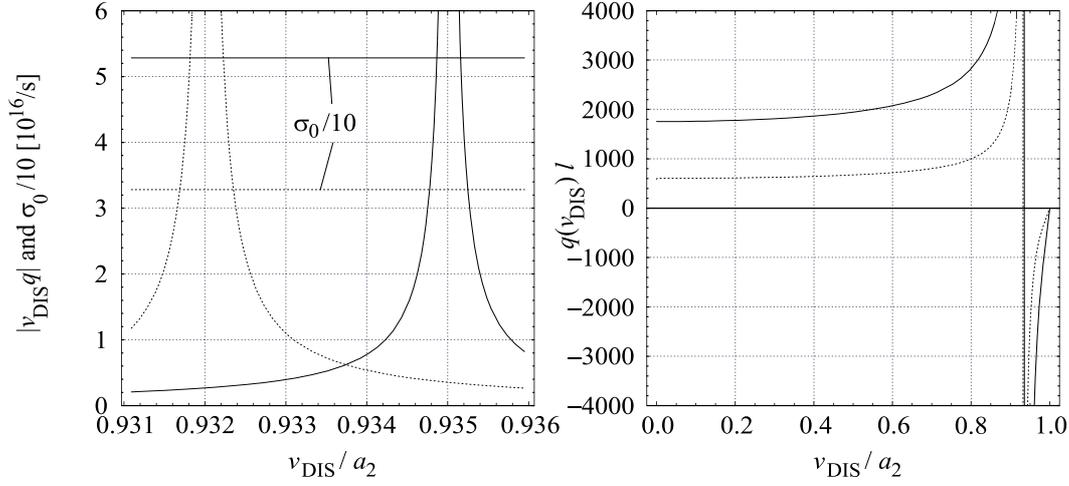
FIGURE 3.3–3 Velocity-dependence of the conditions of equation (3.3–35) for Cu (solid lines) and Al (dashed lines). Left: comparison of $v_{DIS}q$ and $\sigma_0/10$, where $v_{DIS}q$ should be smaller than σ_0. The interval of the dislocation velocity is taken very close around the Rayleigh velocities of Cu and Al. Right: The product ql. In this case, the condition that should be fulfilled is $ql \gg 1$.

played in figure 3.3–2. In both cases of edge and screw dislocation, the width of the core decreases with increasing dislocation velocity, in case of an edge dislocation even turning negative at the Rayleigh velocity v_R (equation (2.3–14)). The interpretation of this phenomenon is discussed elsewhere[25,26], but the use of linear elasticity to describe the core width in that region is at least questionable. In any case, the trend of decreasing core width ζ with increasing dislocation velocity v_{DIS} increases the magnitude of the typical Fourier component q, thereby strengthening the condition $ql \gg 1$.

The product $|q(v_{DIS})v_{DIS}|$ and the conductivity $\sigma_0/10$ are plotted in figure 3.3–3 for Cu and Al. The product becomes comparable in magnitude to $\sigma_0/10$ (where the factor 10 is chosen to denote the "much larger" of conditions (3.3–35)) only well within the region $(v_{DIS} \pm v_R)/v_R < 0.1\%$, very close to the Rayleigh velocity. Outside of this region, the condition $|\vec{q} \cdot \vec{v}_{DIS}| \leq |q(v_{DIS})v_{DIS}| \ll \sigma_0$ is easily satisfied. We are now on safe grounds to put the velocity-dependent dilatation into equation (3.3–31). According to equations (2.2–12), (2.2–13), (2.3–15) and (3.3–32), the dilatation is

$$\Delta(v_{DIS}) = -\frac{b}{\pi}\frac{1-2\nu}{2-2\nu}\frac{\beta_1 x_2}{\left(x_1 - v_{DIS}t\right)^2 + \beta_1^2 x_2^2} \tag{3.3–39}$$

and its two-dimensional Fourier transform reads

$$\Delta_q(v_{DIS}) = \frac{2b}{V}\left(\frac{1-2\nu}{1-\nu}\right)\frac{\sin\left(\frac{1}{2}q_3 L\right)}{iq_3}e^{-iv_{DIS}tq_1}\frac{q_2}{\beta_1^2 q_1^2 + q_2^2}, \tag{3.3–40}$$

which reduces to equation (3.3–33) when $v_{DIS} \to 0$. Is it instructive to look at the velocity-dependent part

$$\frac{\left|\Delta_q\left(v_{DIS}\right)\right|^2}{\left|\Delta_q(0)\right|^2} = \left(\frac{q_1^2 + q_2^2}{\beta_1^2 q_1^2 + q_2^2}\right)^2, \tag{3.3–41}$$

which has its maximum value along $q_2 = 0$, for which it reduces to β_1^{-4} (except for $q_1 = 0$, when it becomes 1 everywhere). This term becomes arbitrarily large when $v_{DIS} \to a_1$. However, the maximum velocity for an edge dislocation is only a_2 ($a_1/2$ for $v = 1/3$), and conditions (3.3–35) are only valid up to the Rayleigh velocity v_R. The maximum value of the velocity-dependent part is therefore attained for $q_2 = 0$, $q_1 \neq 0$ and $v_{DIS} = v_R$, for which it is 1.63 ($v = 1/3$), so the velocity-dependence of the dilatation changes the electron drag coefficient by less than an order of magnitude. We will further discuss this in section 3.3.4, where the relative importance of the various damping mechanisms will be discussed.

3.3.3 IMPURITY VISCOSITY

The interaction energy W of a solute atom and a stationary edge dislocation is well described in literature[27]. Here we are interested whether impurities contribute to the damping of fast-moving dislocations. The flow of solute atoms, J, is proportional to the concentration c and the gradient of the interaction energy W:

$$J \sim c\nabla W. \tag{3.3–42}$$

For stationary dislocations the solute atoms follow a circular trajectory. When the dislocation is moving with a velocity v_{DIS} an apparent flow relative to the dislocation is added, leading to

$$J_D = -\frac{D_C}{k_B T} c\nabla\left(W_{static} + \frac{k_B T v_{DIS}}{D_C} x_1\right). \tag{3.3–43}$$

This flow is the same for a stationary case provided the interaction energy is changed to

$$W_{moving}\left(v_{DIS}\right) = W_{stat} + \frac{k_B T v_{DIS}}{D_C} x_1. \tag{3.3–44}$$

W_{static} is given by (in polar coordinates with $\theta = x_2/r$)[27]
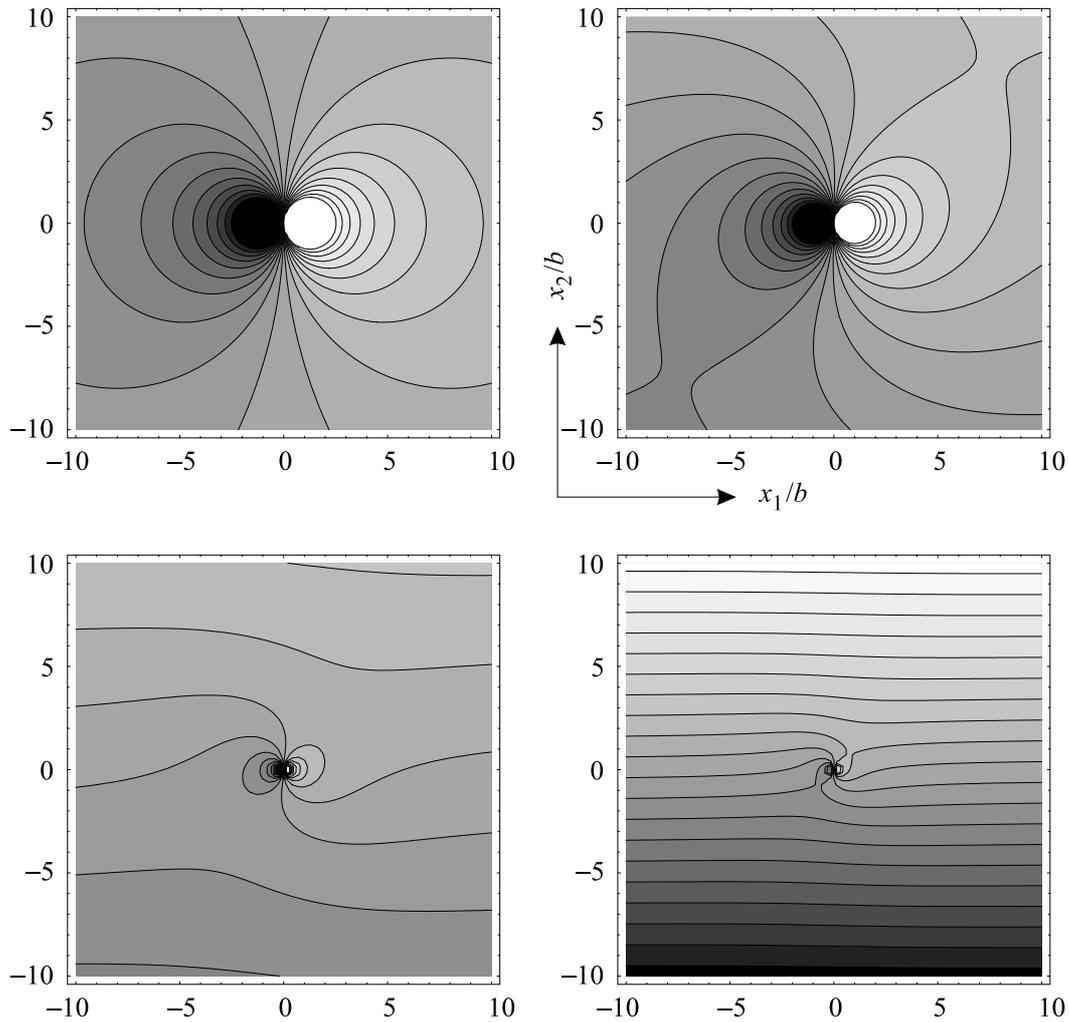
FIGURE 3.3–4 Flow lines between $-10 < x_1/b < 10$ and $-10 < x_2/b < 10$ for C-solutes in Fe along the gradients of the stress field of a dislocation, which is located at the centre. Top left: $v_{DIS} = 0$ m/s. Top right: $v_{DIS} = 10^{-21}$ m/s. Bottom left: $v_{DIS} = 10^{-20}$ m/s. Bottom right: $v_{DIS} = 10^{-19}$ m/s. In all cases $T = 300$ K.

$$W_{static} = \frac{3\mu b\Omega\varepsilon_a}{\pi}\frac{\sin\theta}{r} \equiv A\frac{\sin\theta}{r}, \qquad (3.3\text{–}45)$$

where $\varepsilon_a = d(\ln a_L)/dc$ with a_L the lattice constant, and Ω denotes the atomic volume. The equation for the flow lines, based on equation (3.3–44) now becomes

$$A\frac{x_1}{x_1^2 + x_2^2} + \frac{k_B T}{D_C}v_{DIS}x_2 = \eta. \qquad (3.3\text{–}46)$$

Figure 3.3–4 shows the flow lines for a static dislocation, and for a dislocation that is moving *very* slowly. Below a certain critical η_C the flow lines have one end at the core of the dislocation. Above a critical value of (for which $v_{DIS} = v_C$)

$$\eta_C = \sqrt{\frac{2Ak_BT\,v_C}{D_C}} \; ,$$

(3.3–47)

we have *open* flow lines, which do not go through the dislocation core and *closed* flow lines, both ends of which are at the core. The critical distance away from the slip plane where the solute atoms always flow away from the core is given by

$$\left. y \right|_{\mathrm{crit}} = \frac{1+\sqrt{2}}{\eta_C}A, \quad \text{or} \quad \left. y \right|_{\mathrm{crit}} = \left(1+\frac{1}{\sqrt{2}}\right)\sqrt{\frac{AD_C}{k_BT\,v_{DIS}}} \; .$$

(3.3–48)

The reason for a solute atmosphere being formed is that there are flow lines ending at the dislocation core. Consequently, *no* solute atmosphere will be formed if the dislocation is moving so fast that, say,

$$\left. y \right|_{\mathrm{crit}} < b, \quad \text{or} \quad v_C > \frac{3+2\sqrt{2}}{2}\frac{AD_C}{b^2k_BT} .$$

(3.3–49)

In figure 3.3–5 this is displayed for C in Fe as a function of temperature. Note that D_C depends critically on temperature and activation energy through[28]

$$D_C = D_{C,0}\,e^{-\frac{Q}{RT}} ,$$

(3.3–50)

where $D_{C,0}$ is not dependent on temperature, Q denotes the activation energy for interstitial diffusion and $R = 8.3$ J mol^{-1} K^{-1}. Note that in this case, even at high temperatures, v_C is of the order 10^{-3} to 10^{-2} m/s, which is *very* easily reached at the strain rates of interest.

When the dislocation is moving with $v_{DIS} < v_C$, a solute atmosphere will be formed and a concentration gradient is produced. The force from all the solute atoms is given by

$$\vec{F} = -\int_V \frac{c}{\Omega}\nabla W \,\mathrm{d}V ,$$

(3.3–51)

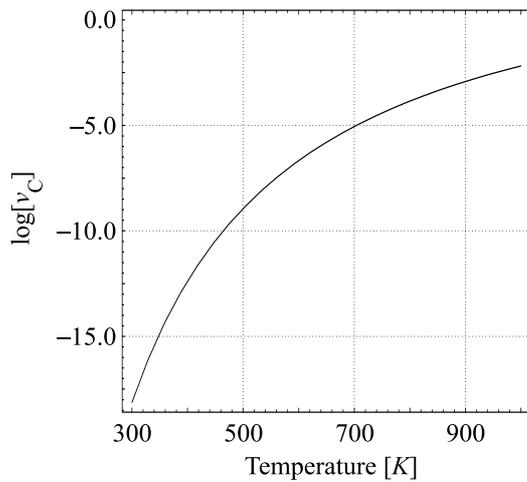and the magnitude of the drag force per unit length can then be defined as

FIGURE 3.3–5 Temperature dependence of the critical velocity v_C above which C-solutes in Fe cannot reach the core of the moving dislocation, according to equations (3.3–49) and (3.3–50).

$$F_{\text{DRAG}} = -\int_V \frac{c \nabla W}{\Omega} \, d\vec{s} \cdot \left(\frac{\vec{v}_{\text{DIS}}}{v_{\text{DIS}}} \right) \tag{3.3–52}$$

per unit dislocation length in the direction of v_{DIS}. Analytical solutions of (3.3–52) are difficult to obtain[29]. For *small* v_{DIS}, B_{IMP} is given by

$$B_{\text{IMP}} \cong \frac{17}{4} \frac{A^2 c_0}{D_C \, k_B T \, \Omega}, \tag{3.3–53}$$

with c_0 the equilibrium concentration, while for $v_{\text{DIS}} > v_C$, $B_{\text{IMP}} = 0$.

3.3.4 SUMMARY AND DISCUSSION

The three contributions to the drag coefficient that have been mentioned in equation (3.3–3) and that have been developed in the last few sections can now be put together to give the overall drag coefficient B_{TOT} according to

$$B_{\text{TOT}} = B_{\text{PH}} + B_{\text{E}} + B_{\text{IMP}} = B_{\text{wind}}^0 + B_{\text{slow}}^0 + B_{\text{flut}} + B_{\text{E}} + B_{\text{IMP}}. \tag{3.3–54}$$

It has been noted[11,12] that the velocity-*independent* theories leading to (3.3–53) are very successful in the prediction of the variation with temperature dependence of $B(T)/B(\theta_D)$ at not too low temperatures, and of the relative contribution of each of the components. However, the prediction of the *absolute value* of B has in some cases been met with success but with failure in some others. For instance in Cu, where the experimental value for edge dislocations lies between 17 and 20 μPa s at room temperature, the theoretical temperature dependence quite accurately pre-

dicts the experimental values. The same holds for the values of Al at temperatures above 100 K (B_{TOT} lies between 24 and 57 μPa s at room temperature), but in the very low temperature regime, the experimental data show an increase with decreasing temperature, opposite to the predictions of the theories presented here. An extended discussion of these issues (with references to experimental data) is given in Nadgornyi[11].

In our case, however, the main interest is in the *velocity*-dependence of B_{TOT}, especially in the high velocity regime, which was not treated in literature extensively. Of relevance here is that we will use the available experimentally determined values, and evaluate the components of equation (3.3−54) to give their *relative* contribution to the total drag. Specifically, it is of interest to determine the relative contributions of B_{flut} and B_E, since these are the contributions with a velocity-dependence.

Starting with the electronic contribution, we have already seen that its static value is typically of the order of 1 μPa s or below for Cu and Al. In the limit $v_{DIS} \rightarrow v_R$, these values increase at most by a factor of 1.6, so even in the high velocity-limit, the order of magnitude remains around 1 μPa s. Compared with the magnitude of the total drag coefficients in these metals, they may safely be neglected, except at very low temperatures. This is not the case with the flutter mechanism, since it becomes arbitrarily large when $v_{DIS} \rightarrow a_2$. At not too low temperatures, we define

$$B_{TOT}\left(v_{DIS}\right) = B_{static} + B_{dynamic}\left(v_{DIS}\right) \approx B_{flut}^{0}\left(\frac{B_{static}}{B_{flut}^{0}} + \frac{1}{1-\left(v_{DIS}/a_2\right)^2}\right), \quad (3.3-55)$$

where

$$B_{static} = B_{wind}^{0} + B_{slow}^{0} \left(= B_{PH}^{static}\right) \quad (3.3-56)$$

collects all velocity-*in*dependent terms. The contribution B_{IMP} has been neglected in the dynamic term, the reasons for which have been explained in the previous section. Al'shitz et al.[12] calculated the ratios between the various phonon contributions. At $T = \theta_D$, they found $B_{wind}^{0}/B_{flut}^{0} \sim 10$, $B_{wind}^{0}/B_{slow}^{0} \sim 1$.

The exact values of these ratios depend on the values of the anharmonicity constants α and α_G in the expressions for the phonon wind en slow phonon drag. Unfortunately, the α's have been calculated for only a few cases. In those cases, we will use the previously mentioned estimates. For Cu, the anharmonicity constants are known[30,31], yielding $B_{wind}^{0}/B_{flut}^{0} = 20$ for $T \geq \theta_D$ and $(T/50)^2$ for $T \ll \theta_D$.

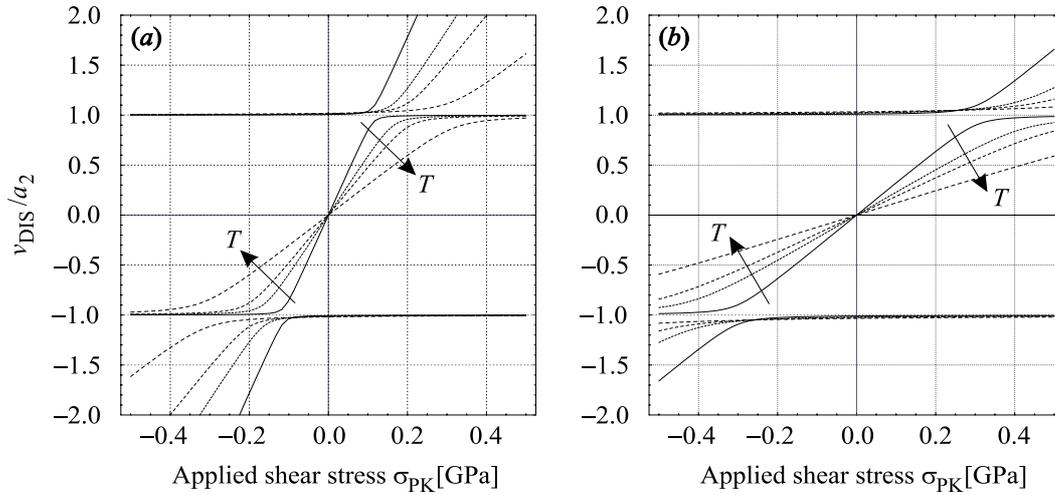Substituting the total drag coefficient B_{TOT} into equation (3.3−2) leads to

FIGURE 3.3–6 Stress-velocity relation for (*a*) Cu ($a_2 = 2.1$ km/s) and (*b*) Al (with $a_2 = 3.1$ km/s). The three curves are solutions of equation (3.3–58). The continuous line denotes the cases for which $T = 100$ K, the dotted line $T = 298$ K and the dashed lines $T = 450$ K and $T = 900$ K. The direction of *in*creasing temperature is also indicated by arrows.

$$\sigma_{\text{PK}} b = B_{\text{TOT}} v_{\text{DIS}} = \left(B_{\text{static}} + \frac{B_{\text{flut}}^0}{1 - v_{\text{DIS}}^2 / a_2^2} \right) v_{\text{DIS}}. \qquad (3.3\text{–}57)$$

The dislocation velocity in the steady state is then given by the solution of

$$\left(\frac{v_{\text{DIS}}}{a_2} \right)^3 - \frac{\sigma_{\text{PK}} b}{a_2 B_{\text{static}}} \left(\frac{v_{\text{DIS}}}{a_2} \right)^2 - \frac{B_{\text{static}} + B_{\text{flut}}^0}{B_{\text{static}}} \left(\frac{v_{\text{DIS}}}{a_2} \right) + \frac{\sigma_{\text{PK}} b}{a_2 B_{\text{static}}} = 0. \qquad (3.3\text{–}58)$$

This equation has three real solutions only if the coefficients fulfil certain criteria, which is the case here. The solutions are not written down here, since they are rather lengthy, but they are plotted for Cu and Al in figure 3.3–6 over a wide range of stresses σ_{PK} between -1 and 1 GPa, and for temperatures of 100 K, 298 K 450 K and 900 K. Of the three solutions, only one gives $-a_2 < v_{\text{DIS}} < a_2$, while for the other two $|v_{\text{DIS}}| > a_2$. Note that figure 3.3–6*a* and 3.3–6*b* are *not* normalised to the same shear wave velocity a_2: $a_2^{\text{Cu}} = 2.1$ km/s and $a_2^{\text{Al}} = 3.1$ km/s. For a given applied shear stress, it can been seen that the resulting dislocation velocity *de*creases with *in*creasing temperature.

§3.4 RELATIVISTIC REGIME

Let's return to the second possibility to "hold a dislocation back" (equation 3.1–13), namely to increase the dislocation mass with increasing velocity causing the acceleration to decrease. The acceleration of a dislocation can be calculated

without much difficulty. Taking into account the inertial term that was neglected in the force balance on the dislocation line (equation (3.3–2)) yields

$$\vec{F}_{\text{Peach-Köhler}} - \vec{F}_{\text{drag}} - \vec{F}_{\text{bowing}}(r) - \frac{\text{d}}{\text{d}t}(m\vec{v}) = 0 , \qquad (3.4–1)$$

with r the bow-out radius of the dislocation line. Again assuming that we deal with straight edge dislocations, the bowing term vanishes. The rest mass $m_{\text{s},0}$ per unit length of a *screw* dislocation follows from the definition of the elastic self-energy

$$\frac{\mu b^2}{4\pi} \ln\left(\frac{R}{r_0}\right) = m_{\text{s},0} a_2^2 = m_{\text{s},0}\left(\frac{\mu}{\rho}\right), \qquad (3.4–2)$$

or

$$m_{\text{s},0} = \frac{\mu b^2}{4\pi a_2^2} \ln\left(\frac{R}{r_0}\right) = \frac{\rho b^2}{4\pi} \ln\left(\frac{R}{r_0}\right). \qquad (3.4–3)$$

with μ the shear modulus, ρ the material density, r_0 and R cut-off radii for the core and the crystal surface, respectively. Usually, r_0 is taken as b and R such that $m_{\text{s},0} \cong \rho b^2$. Weertman[26] noted, in analogy to Einstein's relativity theory, that

$$m_{\text{s}} = \frac{m_{\text{s},0}}{\beta_2} . \qquad (3.4–4)$$
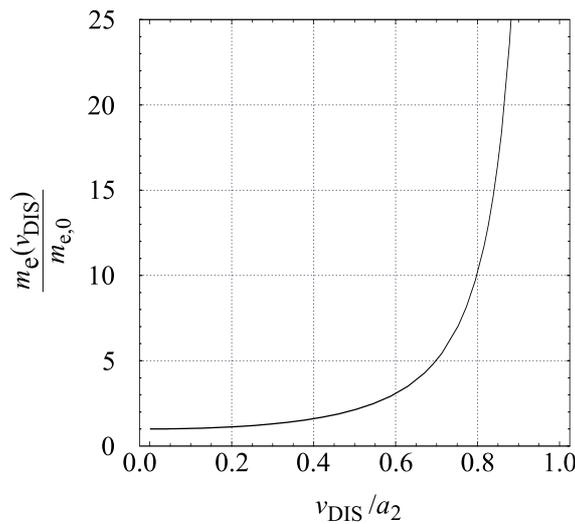

FIGURE 3.4–1 Relative mass with respect to the static value $m_{\text{e},0}$ of an edge dislocation moving at a velocity $0 \leq v_{\text{DIS}}/a_2 < 1$ in the x_1-direction, according to equations (3.4–7) and (3.4–8), for $\nu = 1/3$.

Differentiating m_s with respect to the time, t yields

$$\frac{dm_s}{dt} = \frac{d(m_{s,0}/\beta_2)}{dv_{DIS}}\frac{dv_{DIS}}{dt} = \frac{m_{s,0}v_{DIS}}{a_2^2\beta_2^3}\frac{dv_{DIS}}{dt}.$$

(3.4–5)

Substitution of equation (3.4–4) into (3.4–1) reads

$$\sigma_{PK}b - Bv_{DIS} = \frac{m_{s,0}}{\beta_2^3}\frac{dv_{DIS}}{dt} = \frac{m_{s,0}}{\beta_2^3}a.$$

(3.4–6)

The acceleration of a screw dislocation Cu at $\sigma_{PK} = 100$ MPa from rest lies in the range of 10^{13} m/s^2.

As already noted by Weertman, for a gliding *edge* dislocation, the analogy with Einstein's relativity theory breaks down. As Hirth et al.[32] briefly reviewed, several self-consistent definitions for the velocity-dependence of the dislocation mass may be defined. For the edge dislocation, they argue in favour of

$$m_e(v_{DIS}) = m_{s,0}\left(\frac{a_2}{v_{DIS}}\right)^4\left(-8\beta_1 - \frac{20}{\beta_1} + \frac{4}{\beta_1^3} + 7\beta_2 + \frac{25}{\beta_2} - \frac{11}{\beta_2^3} + \frac{3}{\beta_2^5}\right).$$

(3.4–7)

The relative mass of a moving *edge* dislocation is plotted in figure 3.4–1. In the static limit, the "rest mass" of an edge dislocation reduces to

$$m_{e,0} = m_{s,0}\left(1 + \left(\frac{a_2}{a_1}\right)^4\right) = m_{s,0}\left(1 + \left(\frac{1-2\nu}{2-2\nu}\right)^2\right).$$

(3.4–8)

The expressions (3.4–1) and (3.4–7) will be used in Chapter 4 to determine whether the inertial term plays a significant role, and if so, to determine the regime of velocities, temperatures and time increments in which it might be the case.

§3.5 CONCLUDING REMARKS

In this chapter we have delineated three regimes −thermally activated glide, drag controlled and relativistic motions− to describe dislocation dynamics from $v_{DIS} = 0$ to $v_{DIS} = a_2$. It is appropriate to make some connections with constitutive equations and macroscopic predictions. First, the *macroscopic* strain rate in the constitutive equation (3.1–5) can be connected to the static dislocation drag coefficient by the Orowan equation (3.2–2):

$$\dot{\gamma} = \rho_{\mathrm{M}} b \bar{v}_{\mathrm{DIS}} = \frac{\rho_{\mathrm{M}} b^2 \tau_{\mathrm{D}}}{B_{\mathrm{TOT}}(\bar{v}_{\mathrm{DIS}})} \cong \frac{\rho_{\mathrm{M}} b^2 \tau_{\mathrm{D}}}{B_{\mathrm{TOT}}(0)}, \tag{3.5-1}$$

where it is assumed that the *average* velocity remains low enough so that the corresponding drag coefficient can be approximated by its static value $B_{\mathrm{TOT}}(0)$, according to equation (3.3−55). In addition, the drag force has been written as $\tau_{\mathrm{D}} b$ in a similar fashion as equation (3.3−2). Furthermore, if the a-thermal resistance due to inter-dislocation interaction is expressed as the internal stress[33]

$$\tau_i = \alpha \mu b \sqrt{\rho_{\mathrm{TOT}}}, \tag{3.5-2}$$

with $\alpha = 1/3$ for forest dislocations, then the flow stress is expressed as

$$\tau = \alpha \mu b \sqrt{\rho_{\mathrm{TOT}}} + \frac{B_{\mathrm{TOT}}(0)\dot{\gamma}}{b^2 \rho_{\mathrm{M}}}. \tag{3.5-3}$$

The effective stress (2nd term) decreases with increasing mobile dislocation density and the internal stress (1st term) increasing with the total or forest dislocation density[10]. The flow stress becomes a minimum at a critical value of ρ_{C}:

$$\rho_{\mathrm{C}} = \left(\frac{8 B_{\mathrm{TOT}}(0)\dot{\gamma}}{\alpha \mu b^3} \right)^{2/3}, \tag{3.5-4}$$
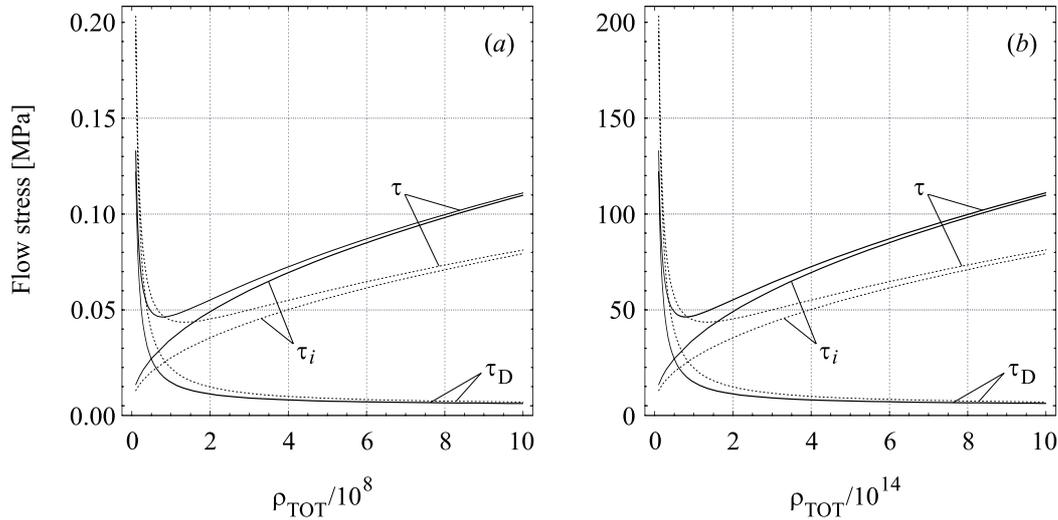

FIGURE 3.5−1 Flow stress τ in Cu (solid lines) and Al (dashed lines) according to equation (3.5−3), with $\alpha = 1/3$ for forest dislocations. (*a*) $\dot{\gamma} = 10^{-3}\,\mathrm{s}^{-1}$. (*b*) $\dot{\gamma} = 10^6\,\mathrm{s}^{-1}$. The lines running from the origin denote τ_i (equation (3.5−2)), the lines converging towards the horizontal axes with increasing ρ_{TOT} denote τ_{D} from equation (3.5−1) and the remaining lines denote their sum (equation (3.5−3)). The total flow stress attains its minimum for $\rho = \rho_{\mathrm{C}}$ (equation (3.5−4)).
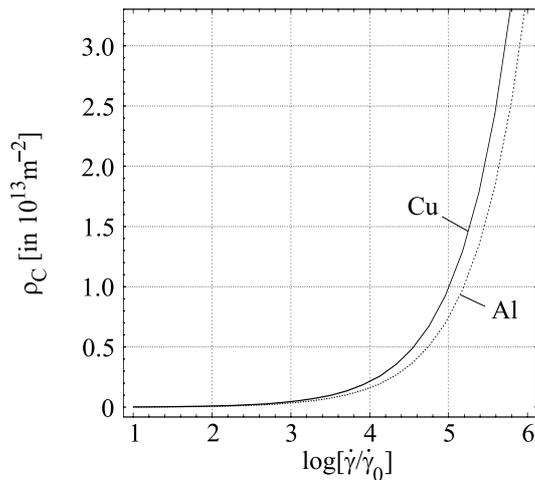
FIGURE 3.5–2 Critical dislocation density ρ_C in Cu and Al according to equation (3.5–4).

with[10] $\rho_M = \rho_{TOT}/4$. The critical density is shown in figures 3.5–1 and 3.5–2. Defining ρ_U as the steady state density and ρ_0 as the initial dislocation density, it is clear that work-hardening occurs if $\rho_0 > \rho_C$, and first work softening and then work hardening for $\rho_0 < \rho_C < \rho_U$. The critical density is proportional to $\left(\dot{\gamma}B\right)^{2/3}$ and therefore we expect work softening to occur if the dislocation drag coefficient increases (due to relativistic effects in the phonon term or a temperature change in the phonon- or impurity term) and/or if the strain rate increases.

§3.6 LITERATURE

1. JOHNSON G.R., HOEGFELDT J.M., LINDHOLM U.S., NAGG A., ASME J. Eng. Mater. Tech. **105** (1983), 42.
2. MUNZ D., FETT T., *Ceramics*, Springer Verlag, Berlin (1998).
3. ANDRADE U.R., MEYERS M.A., CHOKSHI A.H., *Constitutive description of work- and shock-hardened Copper*, Scripta Mat. **30** (1994), 933 and MEYERS M.A., *Dynamic behaviour of materials,* Wiley, New York (1994), 323.
4. CAMPBELL J.D., ELEICHE A.M.E., TSAO M.C.C., *Fundamental aspects of alloy design*, Plenum, New York (1977), 545.
5. JOHNSTON W.G., GILMAN J.J., *Dislocation velocities, dislocation densities and plastic flow in LiF crystals*, J. Appl. Phys. **30** (1959), 129.
6. POPE D.P., VREELAND T., WOOD D.S., *Mobility of edge dislocations in the basal slip system of Zinc*, J. Appl. Phys. **38** (1967), 4011.
7. GREENMAN W.F., VREELAND T., WOOD D.S., *Dislocation mobility in Copper*, J. Appl.Phys. **38** (1967), 3595.
8. GILMAN J.J., *Micromechanics of flow in solids*, McGraw-Hill, New York (1969), 179.
9. KOCKS U.F., ARGON A.S., ASHBY M.F., *Thermodynamics and kinetics of slip*, Progress in Materials Science **19** , Pergamon (1975).

10. DE HOSSON J.TH.M., KANERT O., SLEESWIJK A.W., review in *Dislocations in Solids* (ed. NABARRO F.R.N.), North Holland Publ. Comp., Vol **6** (1983), 441.

11. NADGORNYI E., *Dislocation dynamics and mechanical properties of crystals*, Progress in Materials Science **31**, Pergamon (1988).

12. AL'SHITZ V.I., INDENBOM V.L., *Dynamic dragging of dislocations*, Soviet Physics Uspekhi **18** (1975), 1.

13. BRAILSFORD A.D., *Anharmonic dislocation drag*, J. Appl. Phys. **43** (1972), 1380.

14. LOTHE J., *Theory of dislocation mobility in pure slip*, J. Appl. Phys **33** (1962), 2116.

15. NABARRO F.R.N., *Theory of crystal dislocations*, Oxford 1967, Chapter 7.

16. NINOMIYA T., *Dislocation vibration and phonon scattering*, J. Phys. Soc. Japan **25** (1968), 830.

17. KOGURE Y., HIKI Y., *Lattice thermal conductivity of crystals containing dislocations*, J. Phys. Soc. Japan **38** (1975), 471.

18. KLEMENS P.G., *Thermal conductivity and lattice vibration modes*, Solid State Physics (eds. SEITZ F., TURNBULL D.) **7**, Acad. Press, New York (1958), 1.

19. GILLIS P.P., GILMAN J.J., TAYLOR J.W., *Stress depencences of dislocation velocities*, Phil. Mag. **20** (1969), 279.

20. TITTMANN B.R., BÖMMEL H.E., *Amplitude-dependent ultrasonic attenuation in superconductors*, Phys. Rev. **151** (1966), 178.

21. SEEGER A., WESOLOWSKI Z., *Physics of strength and plasticity* (ed. ARGON A.S.), MIT Press, Cambridge Mass. (1965), 15.

22. BRAILSFORD A.D., *Electronic component of dislocation drag in metals*, Phys. Rev. **186** (1969), 959.

23. KITTEL C., *Quantum theory of Solids*, Wiley, New York (1963), Chapter 17.

24. KITTEL C., *Introduction to Solid State Physics* (6th ed.), Wiley, New York (1986). GRUNER, P.Z., BROSS, Phys. Rev. **172** (1968), 583

25. ESHELBY J.D., *Uniformly moving dislocations*, Proc. Royal Soc. **A62** (1949), 307.

26. WEERTMAN J., WEERTMAN J.R., *Moving dislocations*, in *Dislocations in Solids* (ed. NABARRO F.R.N.), North-Holland Publishing Comp. (1980), Chapter 8.

27. HIRTH J.P., LOTHE J., *Theory of dislocations*, Wiley, New York (1982).

28. PORTER D.A., EASTERLING K.E., *Phase transformations in Metals and Alloys* (2nd ed.), Chapman & Hall, London (1992).

29. COTTRELL A.H., JASWON M.A., *Distribution of solute atoms round a slow dislocation*, Proc. R. Soc. London **A199** (1949), 104. YOSHINAGA,H., MOROZUMI, S, Phil. Mag. **23** (1971), 1351.

30. AL'SHITZ V.I., Soviet Phys. Solid State **11** (1970), 1947.

31. AL'SHITZ V.I., MITLIANSKII M.D., KOTOWSKI R.K., Arch Met. **31** (1974), 91.

32. HIRTH J.P., ZBIB H.M., LOTHE J., *Forces on high velocity dislocations*, Modelling Simul. Mater. Sci. Eng. **6** (1998), 165.

33. HIRSCH P.B., *Work hardening*, in *The physics of metals* (ed. HIRSCH P.B.), Vol. **2**, Cambridge University Press, London (1975).